Systems-wide analysis of the ROK-family regulatory gene *rokL6* and the control of aminosugar toxicity in *Streptomyces coelicolor*

Chao Li[a], Mia Urem[b], Chao Du[a], Le Zhang[a], Gilles P. van Wezel[a*]

[a] Molecular Biotechnology, Leiden University, PO Box 9505, 2300RA Leiden, The Netherlands

[b] Department of Human Genetics, Leiden University Medical Center, Leiden, The Netherlands

ABSTRACT

Streptomycetes are saprophytic bacteria that grow on complex polysaccharides, such as cellulose, starch, chitin and chitosan. For the monomeric building blocks glucose, maltose and *N*-acetylglucosamine (GlcNAc), the metabolic pathways are well documented, but that of glucosamine (GlcN) is largely unknown. *Streptomyces nagB* mutants, which lack glucosamine-6-phosphate deaminase activity, fail to grow in the presence of high concentrations of GlcN. Here we report that mutations in the gene for the ROK-family transcriptional regulator RokL6 relieve the toxicity of GlcN in *nagB* mutants, as a result of elevated expression of the Major Facilitator Superfamily (MFS) exporter SCO1448. Systems-wide analysis using RNA sequencing, ChIP-Seq, EMSAs, 5'RACE, bioinformatics and genetics revealed that RokL6 is an autoregulator that represses transcription of SCO1448 by binding to overlapping promoters in the *rokL6*-SCO1448 intergenic region. RokL6-independent expression of SCO1448 fully relieved toxicity of GlcN to *nagB* mutants. Taken together, our data show a novel system of RokL6 as a regulator that controls the expression of the MFS transporter SCO1448, which in turn protects cells against GlcN toxicity, most likely by exporting toxic metabolites out of the cell.

IMPORTANCE

Central metabolism plays a key role in the control of growth and antibiotic production in streptomycetes. Specifically, aminosugars act as signaling molecules that affect development and antibiotic production, via metabolic interference with the global repressor DasR. While aminosugar metabolism directly connects to other major metabolic routes such as glycolysis and cell wall synthesis, several important aspects of their metabolism are yet unresolved. Accumulation of GlcNAc-6P or GlcN-6P is lethal to many bacteria, a yet unresolved phenomenon referred to as “aminosugar sensitivity”. We made use of this concept by selecting for suppressors in genes related to GlcN toxicity in *nagB* mutants, which showed that the gene pair of *rok*-family regulatory gene *rokL6* and MFS transporter gene SCO1448 forms a cryptic rescue mechanism. Inactivation of *rokL6* resulted in the expression of SCO1448, which then prevents toxicity of amino sugar-derived metabolites in *Streptomyces*. The systems biology of RokL6 and its transcriptional control of SCO1448 sheds new light on aminosugar metabolism in streptomycetes and on the response of bacteria to aminosugar toxicity.

KEYWORDS

ROK-family protein; aminosugar metabolism; systems biology; *Streptomyces* biology; control of antibiotic production

INTRODUCTION

Streptomycetes are Gram-positive bacteria with a mycelial lifestyle that reproduce via sporulation. Their large GC-rich genomes encode a plethora of specialized metabolites such as antibiotics, anticancer drugs and many other industrially and medically relevant compounds (1-3). The production of these molecules is closely related to the transition from vegetative to aerial growth during development of the colonies (4, 5). Streptomycetes grow by tip extension and branching of vegetative hyphae, which are divided into multigenomic compartments. Under adverse conditions such as nutrient depletion, a complex developmental program is initiated that results in the formation of an aerial mycelium, and eventually the aerial hyphae differentiate to form chains of unigenomic spores (3, 6). At the onset of development, the vegetative mycelium is partially degraded via programmed cell death (PCD) so as to provide the building blocks necessary for aerial growth in an otherwise nutrient-depleted environment (7, 8).

During cell wall recycling, the constituents of the peptidoglycan (PG), namely *N*-acetylglucosamine (GlcNAc) and *N*-acetylmuramic acid (MurNAc) that make up the PG strands and the cross-linking amino acids, are re-imported into the cell. The lactyl ether substituent of the intracellular MurNAc 6-phosphate (MurNAc-6P) is cleaved by MurNAc-6P etherase (MurQ), yielding *N*-acetylglucosamine 6-phosphate (GlcNAc-6P) (9). GlcNAc is thereby internalized by the phosphoenolpyruvate-dependent phosphotransferase system (PTS) which simultaneously phosphorylates GlcNAc to GlcNAc-6P (10, 11). The next step is GlcNAc-6P deacetylation by *N*-acetylglucosamine 6-phosphate deacetylase NagA forming glucosamine-6-phosphate (GlcN-6P), which is a central molecule at the intersection of multiple metabolic pathways, including glycolysis via conversion to fructose-6-phosphate (Fru-6P) by glucosamine-6-phosphate deaminase NagB (12).

GlcNAc plays a critical role in signaling during the control of development and antibiotic production in streptomycetes (13). Under poor nutritional conditions (*famine*), GlcNAc-6P and GlcN-6P act as allosteric inhibitors of the DNA binding activity of the global regulator DasR (14, 15). DasR controls aminosugar transport and metabolism and is also a highly pleiotropic repressor of antibiotic production in *Streptomyces*, whereby it represses all gene clusters for antibiotics and siderophores in *Streptomyces coelicolor* (14-16). Metabolic control of DasR is a key step in the early activation of development and specialized metabolism under nutrient-deprived conditions. Conversely, on rich media (*feast)*, GlcNAc activates development and antibiotic production, and this phenomenon is less well understood, though iron availability likely plays a role (17, 18).

While the metabolic pathway of GlcNAc has been well characterized, little is known of glucosamine (GlcN) metabolism in streptomycetes. The hydrolysis of chitosan and the metabolism of chitosan-derived oligomers $(GlcN)_{2\text{-}3}$ are under the control of CsnR (19, 20), a repressor from the ROK (Repressors, ORFs and Kinases) family of transcriptional regulators (21). GlcN oligomers are imported via the ABC-transporter complex CsnEFG-MsiK and are then presumably hydrolyzed and phosphorylated by CsnH, a sugar hydrolase, and CsnK, a ROK-family kinase, respectively.

High concentrations of either GlcN or GlcNAc are toxic to *S. coelicolor* in the absence of the enzyme glucosamine-6-phosphate deaminase (NagB). Similar aminosugar sensitivity was also observed for *Escherichia coli* (22, 23). Despite extensive studies focusing on the metabolism of aminosugars, the underlying cause of aminosugar toxicity remains unresolved. Interestingly, when grown in the presence of high concentrations of either GlcN or GlcNAc, *S. coelicolor* Δ*nagB* strains sustain spontaneous second-site mutations that allow the colonies to survive. We previously exploited this principle to identify novel genes related

to GlcN transport and metabolism (12, 24). Spontaneous mutations or deletion of *nagA*, preventing the conversion from GlcNAc-6P to GlcN-6P, relieves the toxicity of both GlcNAc and GlcN to *S. coelicolor nagB* mutants (24). Since NagA is not known to play a role in GlcN metabolism, this points at a caveat in our understanding of aminosugar metabolism. In addition to suppressor mutations in *nagA*, two independent suppressor mutations were found in the gene for ROK-family regulator SCO1447 (RokL6), which relieved toxicity specifically of GlcN but not of GlcNAc. ROK (Repressor, ORF and Kinase) family of proteins often play important roles in the (control of) sugar utilization in bacteria, and these regulators are widespread in streptomycetes (21, 25, 26).

Here, we report on the function of RokL6 by a systems-wide approach, using mutational and transcriptional analysis, and *in vitro* and *in vivo* DNA binding studies. This revealed that the gene product of *rokL6* is a ROK-family regulator that specifically represses the adjacent gene SCO1448. This gene encodes a putative Major Facilitator Superfamily (MFS) transporter, and we propose that it acts as a pump for toxic substances created during challenge of *nagB* mutants with higher concentrations of GlcN.

MATERIALS AND METHODS

Strains, plasmid, and growth conditions

The bacterial strains and plasmids used or constructed in this study are summarized and listed in the Supporting Information Table S1, and all oligonucleotides are described in Table S2. *Escherichia coli* was grown and transformed according to the standard procedures (27), with *E. coli* JM109 serving as the host for routine cloning, and ET12567 (28) used for the isolation of non-methylated DNA for transformation into *Streptomyces*. For protein heterologous expression, *E. coli* BL21(DE3) from Novagen was used. *E. coli* was grown in Luria-Bertani (LB) media in the presence of selective antibiotics as required, with the following final concentrations: ampicillin (100 μg/mL), apramycin (50 μg/mL), kanamycin (50 μg/mL) and chloramphenicol (25 μg/mL). *Streptomyces coelicolor* A(3)2 M145 (29) was obtained from the John Innes Centre strain collection and was the parent of all mutants. *S. coelicolor nagB* mutant Δ*nagB* (24) and GlcN-derived *nagB* suppressor mutant SMG1 (30), have been described previously. All *Streptomyces* media and routine techniques are based on the *Streptomyces* manual (31). Phenotypic characterization of *Streptomyces* mutants was carried out on minimal medium (MM) agar plates with different carbon sources as indicated. Soy flour mannitol (SFM) agar plates were used for preparation of spore suspensions and *E. coli* to *S. coelicolor* conjugations. A mixture of 1:1 yeast-extract malt extract (YEME) and tryptic soy broth (TSBT) liquid media was used to cultivate mycelia for protoplast preparation and genome DNA isolation. Growth curves of *Streptomyces* were performed in liquid cultures containing minimal medium (NMMP) (31) with 1% (w/v) glucose or GlcN as the sole carbon source, and the dry weights of the mycelia were measured at different time points.

Gene knock-out, complementation and overexpression

As basis for the creation of gene deletion mutants we used the unstable multi-copy plasmid pWHM3 (32, 33), as described previously (12). For the *rokL6* knock-out construct, a 1254-bp 5' flanking region and a 1366-bp 3' flanking region were amplified by PCR from the *S. coelicolor* M145 genome, using the primer pairs described in Table S2. The upstream region was cloned as an *Eco*RI-*Xba*I fragment, and the downstream region as an *Xba*I-*Bam*HI fragment, and these two fragments were ligated into pWHM3 from the *Eco*RI and *Bam*HI sites. The apramycin resistance cassette *aac(3)IV*, flanked by *lox*P sites (apra-*lox*P), was subsequently cloned into the engineered *Xba*I sites between the flanks to create *rokL6* knock-out construct pKO-*rokL6*. In the same way, the flanking regions of SCO1448 were cloned into pWHM3 with the apra-*lox*P to produce SCO1448 knock-out vector, pKO-1448. The knock-out constructs were introduced into *S. coelicolor* M145 or its *nagB* mutant. For clean gene knock-out mutants, the apramycin resistance cassette was excised by introduction of pUWLcre, which expresses Cre recombinase (34, 35). The correct recombination event in each of the knock-out mutants was confirmed by PCR.

For *rokL6* complementation, the entire coding region of *rokL6* with its own promoter was amplified from the *S. coelicolor* chromosome. The PCR product was digested with *Xba*I/*Eco*RV and then inserted into pSET152 (36) to obtain *rokL6*-complemented vector pCOM-*rokL6*. This construct was introduced into *nagB*-*rokL6* double mutant Δ*nagB*Δ*rokL6*, and the successfully complemented strains Δ*nagB*Δ*rokL6*-C were selected by apramycin. The empty pSET152 was conjugated in Δ*nagB*Δ*rokL6* to produce Δ*nagB*Δ*rokL6*-E, which was used as a control strain.

For SCO1448 overexpression, a 1212-bp DNA fragment containing SCO1448 was amplified and ligated into pSET152 with the 63-bp highly efficient promoter P30, namely the promoter

SP30 with the 20-bp ribosomal binding site RBS15 (37), to produce SCO1448-overexpressing vector pOE-1448. The pOE-1448 construct was then introduced into Δ*nagB* to obtain the SCO1448 overexpression strain Δ*nagB*SCO1448-O.

$FLAG_3$ tag knock-in by CRISPR

To express FLAG-tagged RokL6 in *S. coelicolor*, the 3×FLAG sequence ($FLAG_3$) was fused to the end of original copy of *rokL6* on genome using codon optimized CRISPR-Cas9 system (38) as described previously (39). Briefly, the spacer sequence (5'- GGCGCCGCGGGCTACCGCTC-3') specific to *rokL6*, located at the end of the coding region, was inserted into the pCRISPomyces-2 plasmid from *Bbs*I sites. Next, the 2263-bp template containing $FLAG_3$ for homology-directed repair (HDR) was made and inserted into the spacer-containing plasmid, resulting in a *rokL6*- $FLAG_3$ knock-in construct designated as pKI-$FLAG_3$. Mutagenesis was done according to the previous study (39). After conjugation of pKI-$FLAG_3$ to *S. coelicolor* A3(2) M145, ex-conjugants were patched on SFM agar plates with 20 ug/ml apramycin, then positive ex-conjugants were patched on antibiotic-free SFM agar plates and grown at 37°C. Spores were collected and checked for loss of construct. Apramycin-sensitive strains were selected for spore collection, and their genomes were checked for desired recombination events. The successful *in situ* $FLAG_3$ knock-in strain was identified as M145-*rokL6*-FLAG. Additionally, *rokL6* with $FLAG_3$ was ligated into pSET152 to generate pCOM-$FLAG_3$ and introduced into the *nagB-rokL6* double mutant for evaluating RokL6-$FLAG_3$ function *in vivo*.

Heterologous expression and purification of His_6-tagged RokL6 protein

For the heterologous expression of *S. coelicolor* RokL6 in *E. coli*, the 1197-bp *rokL6* coding region was amplified from *S. coelicolor* genomic DNA using primer pair RokL6-exp-F/RokL6-

exp-R. The PCR fragment was ligated into pET-28a (+) from *Xho*I and *Nco*I sites, generating expression vector pEX-RokL6. The RoKL6 expression vector was transformed into *E. coli* BL21(DE3), and the expression of C-terminal His_6-tagged RokL6 recombinant protein, RokL6-His_6 was induced by the addition of Isopropyl β-D-1-thiogalactopyranoside (IPTG) at a final concentration of 1 mM when the cell density was reached around an optical density at 600 nm of 0.6, followed by overnight incubation at 16°C. Cells were harvested, washed, and disrupted in lysis buffer (40) by sonication. Soluble RokL6-His_6 was purified from the supernatant using HisPur Cobalt Resin (Thermo fisher scientific; USA) and dialyzed against EMSA binding buffer.

Chromatin immunoprecipitation sequencing (ChIP-Seq) of RokL6

ChIP-seq experiments were essentially carried out as described previously (39). In brief, *S. coelicolor* M145-*rokL6*-FLAG was grown on MM agar covered with cellophane disks, using mannitol with and without 50 mM GlcN as the carbon source. Mycelia were collected after 24 h (vegetative growth) and 48 h (sporulation). Mycelia were treated with phosphate-buffered saline (PBS) buffer containing 1% formaldehyde for 20 min to cross-link the DNA and protein. After thorough washing in PBS, mycelia were resuspended in lysis buffer (10 mM Tris-HCl pH 8.0, 50 mM NaCl, 15 mg/mL lysozyme, 1× protease inhibitor (Roche, Bavaria, Germany)) and incubated at 37°C for 20 min. After incubation, 0.5 mL IP buffer (100 mM Tris-HCl pH 8.0, 250 mM NaCl, 0.8% v/v Triton-X-100) was added to the mycelia samples, and chromosomal DNA was sheared to 100-500 bp fragments using the Bioruptor Pluswater bath sonication system (Diagenode, Liège, Belgium). Lysates were incubated with 40 µL Anti-FLAG M2 affinity gel (cat A2220, Sigma-Aldrich, St. Louis, US) and incubated at 4°C overnight. After centrifugation, the pellet and untreated total extracts (control) were incubated in 100 µL IP

elution buffer (50 mM Tris-HCl pH 7.5, 10 mM EDTA, 1% m/v SDS) at 65°C overnight to reverse the cross-link. The beads were removed by centrifugation before DNA isolation by phenol-chloroform. The extracted DNA samples were then further purified with the DNA Clean & Concentrator kit (Zymo Research, California, US). The enriched DNA samples were sent to Novogene Europe (Cambridge, UK) for library construction and next-generation sequencing. ChIP-Seq data analysis was performed as described previously (39).

RNA isolation, RNA sequencing (RNA-Seq) and quantity PCR (qPCR)

Spores of 10^7 CFU of *S. coelicolor* M145 and the *rokL6* deletion strain Δ*rokL6* were plated on MM agar plates containing 1% mannitol, or 1% mannitol with 50 mM GlcN. Biomass from two time points (24h on mannitol and 26h on mannitol with GlcN for vegetative growth phase, VEG; and 42h on mannitol and 44h on mannitol with GlcN for sporulation phase, SPO) was collected and snap-frozen in liquid N_2. After breaking the mycelia using a TissueLyser II (Qiagen, Venlo, The Netherlands), the RNA was extracted using a modified Kirby mix (31). The transcriptome sequencing library preparation and sequencing were outsourced to Novogen Europe (Cambridge, UK). Removal of rRNA from the samples was carried out using NEBNext Ultra directional RNA library prep kit (NEB, MA). Sequencing libraries were generated using the NEBNext Ultra RNA library prep kit for Illumina (NEB), and sequencing was performed on an Illumina NovaSeq 6000 platform. Raw data were cleaned using fastp v0.12.2 (41), and then mapped to the *S. coelicolor* M145 genome DNA (GeneBank accession AL645882.2) using bowtie2 v2.4.4 (42). Read counts for each gene were generated by featureCounts v2.0.1 (43). Values for transcripts per million (TPM) were generated using a custom python script. Differentially expressed genes and log2Foldchange were determined using DESeq2 v1.32.0 (44) with the data shrinkage function “apeglm” (45).

For quantitative PCR (qPCR), cDNA was synthesized using the iScript cDNA Synthesis Kit (Biorad, California, US). Briefly, qPCR was performed using the iTaq Universal SYBR green qPCR Kit (Biorad, California, US), and the program used was set as follows: 95°C 30 s; 40 cycles of 95°C 10 s, 60°C 30 s, plate reading; melting curve from 65°C to 95°C with 5 s per 0.5°C increment. The principal RNA polymerase σ factor encoding gene, *hrdB* (SCO5820), was used as the inner control, and the qPCR data was analysed by CFX Manager software (version 3.1, Biorad, California, US), using ΔΔCq standard which is an implementation of the method described by (46).

Electrophoretic Mobility Shift Assays (EMSAs)

EMSA were performed as described previously (39). Double stranded DNA probes (60-bp) were generated by gradually cooling reverse complemented single-strand oligonucleotides in 30 mM HEPES, pH 7.8, heating to 95°C for 5 min, then ramping to 4°C at a rate of 0.1°C/sec. The *in vitro* DNA-protein binding assays were performed in EMSA binding buffer (20 mM HEPES pH 7.6, 30 mM KCl, 10 mM $(NH_4)_2SO_4$, 1 mM EDTA, 1 mM DTT, 0.2% Tween20). The binding reactions (10 µL), including 1 picomole DNA probe, 20 ng/µL BSA, and various concentration of RokL6-His_6, were incubated at 30°C for 20 min. The reactions were then loaded on 5% non-denatured polyacrylamide gels and separated by electrophoresis. The gels were briefly stained with ethidium bromide and imaged using the Gel Doc imaging system (BioRad, California, US).

Determination of transcriptional start sites (TSS)

Transcriptional start sites (TSS) of *rokL6* and SCO1448 were determined by 5' RACE using a 5'/3' RACE Kit 2nd generation (Roche, California, US). Total RNA (2 µg) extracted from 48-

hour cultures of *S. coelicolor* grown on solid minimal medium containing 1% mannitol was used for reverse transcription with gene-specific primers. The obtained cDNA was purified and an oligo(dA) tail added to the 3' end by terminal transferase, followed by PCR amplification of the tailed cDNA with oligo(dT) anchor primer and gene-specific nested primers. Using the resulting PCR product (diluted 1000-fold) as a template, an additional round of PCR was performed with a more inner nested primer and an anchor primer provided in the kit to produce a single specific DNA band. The final PCR product was purified and sent for sequencing, and the TSS was determined as the first nucleotide following oligo(dA).

Promoter activity test

The promoter regions of *rokL6*, SCO1448, *nagKA* (12) and P30 (37) were ligated with a gene expressing enhanced green fluorescent protein (eGFP), and integrated into pSET152 via the *Xba*I/*Eco*RV sites, generating four recombinant vectors: pEGFP-*rokL6*, pEGFP-1448, pEGFP-*nagKA* and pEGFP-P30. The recombinant constructs were then introduced into *S. coelicolor* and *rokL6* deletion mutant Δ*rokL6* to generate the following strains: M145-P*rokL6*-eGFP, M145-P1448-eGFP, M145-P*nagKA*-eGFP, M145-P30-eGFP, and Δ*rokL6*-P*rokL6*-eGFP, Δ*rokL6*-P1448-eGFP, Δ*rokL6*-P*nagKA*-eGFP, Δ*rokL6*-P30-eGFP. The *in vivo* activities of all the promoters were evaluated by comparing the transcription level of the gene for eGFP via confocal microscopy and confirmed by qPCR.

Confocal imaging

Sterile coverslips were inserted into MM with 1% mannitol agar plates at an angle of 45°, and spores of eGFP-harboring strains were inoculated at the intersection angle and

incubated at 30°C for 48 h. The mycelium was scrapped off from coverslips into a drop of water, and then imaged with a TCS SP8 confocal microscope (Leica) using a 63× oil immersion objective (NA: 1.40) (47). Image processing and the analysis of fluorescent intensity were performed using ImageJ (version 1.54d).

Bioinformatics analysis

DNA and protein database searches were performed using the BLAST server of the National Centre for Biotechnology Information (http://www.ncbi.nlm.nih.gov) and the *S. coelicolor* genome page services (http://strepdb.streptomyces.org.uk). Polypeptide sequences were aligned using Clustalw available at http://www.ebi.ac.uk/clustalw. Gene synteny analysis was performed using SynTax (48). To visualize the consensus sequence for the predicted binding site of RokL6, WebLogo (49) was used, and regulon predictions were done using PREDetector (50). The comparative analysis of the intergenic regions of *rokL6*/SCO1448 and their orthologous pairs was performed by MEME (51).

Data availability

Clean RNA-Seq reads and gene read-counts tables are available at GEO database (52) with accession number GSE234437 (https://www.ncbi.nlm.nih.gov/geo/query/acc.cgi?acc=GSE234437). Clean ChIP-Seq reads and binding region identification (peak calling) files are available at GEO database with accession number GSE234438 (https://www.ncbi.nlm.nih.gov/geo/query/acc.cgi?acc=GSE234438).

RESULTS

RokL6 is involved in GlcN metabolism

We previously showed that null mutants of *S. coelicolor nagB* are sensitive to high concentrations of GlcN, whereby spontaneous second-site mutations arise that allow the colonies to survive. Exploitation of this principle led to the identification of suppressor mutations in *nagA* and in a novel gene related to GlcN transport and metabolism (12, 24). Two independent suppressor mutants were obtained in the gene SCO1447 when *S. coelicolor* Δ*nagB* was grown on GlcN, namely SMG1 and SMG38, and these mutations specifically alleviated the toxicity of exclusively on GlcN, but not GlcNAc (24, 53). Suppressor mutant SMG1 had sustained a single nucleotide insertion at nt position 26 within the coding region of SCO1447, while SMG38 had a single nucleotide deletion at nt position 120 in SCO1447. In both cases, the mutations resulted in a frame shift at the beginning of the gene, thereby preventing expression of the active protein. SCO1447 encodes a ROK-family transcriptional regulator which we designated RokL6, based on the terminology that ROK-family proteins are named after the specific cosmid they are located on (25) within the ordered cosmid library that was used for the *S. coelicolor* genome sequencing project (54).

The observation that the mutations specifically alleviate toxicity of GlcN to *nagB* null mutants, but not that of GlcNAc, suggests that RokL6 plays a specific role in (the control of) GlcN metabolism. To test this, the *rokL6* single mutant Δ*rokL6* and *nagB-rokL6* double mutant Δ*nagB*Δ*rokL6* were generated by deleting *rokL6* in *S. coelicolor* M145 and in the previously published *nagB* null mutant (30), respectively. To create the mutants, the entire coding region of *rokL6* (nt positions +3 to + 1200) was replaced with the apramycin resistance cassette *aac(3)IV*, which was flanked by *lox*P sites. The apramycin cassette was subsequently excized from the genome using the Cre recombinase expressed from plasmid

pUWLcre. The resulting *rokL6* single mutant and *nagB-rokL6* double mutant, Δ*nagB*Δ*rokL6*, was confirmed by PCR. In order to ascertain that the phenotypes were specifically caused by the deletion of *rokL6*, we genetically complemented the Δ*nagB*Δ*rokL6* mutant by expressing *rokL6.* For this, the -478/+1226 region of *rokL6*, harboring the entire gene and its promoter region, was amplified from the *S. coelicolor* chromosome and cloned into integrative vector pSET152 to obtain pCOM-*rokL6* (see Materials and Methods for details).

As expected, *S. coelicolor* M145 and its *rokL6* single mutant Δ*rokL6*, which has an intact copy of *nagB*, grew well on all media, while *nagB* mutants were unable to grow on MM with mannitol (1% w/v) and 5 mM GlcN or GlcNAc. The *rokL6-nagB* double mutant grew well on MM with 1% mannitol and 5 mM GlcN, but failed to grow when GlcNAc was used instead of GlcN (Fig. 1). Importantly, transformants expressing RokL6 in the Δ*nagB*Δ*rokL6* double mutant via the introduction of pCOM-*rokL6*, failed to grow, similar to the *nagB* mutant. These data strongly suggest that the deletion of *rokL6* was the sole reason why Δ*nagB*Δ*rokL6* double mutants could grow on GlcN (Fig. 1).

Conservation and gene synteny of *rokL6*

The gene *rokL6* (SCO1447) from *S. coelicolor* consists of 1200 nucleotides (nt) and encodes a protein of 399 amino acids. RokL6 is characterized by an N-terminal winged helix-turn-helix (HTH) DNA-binding site which is found in various families of DNA-binding proteins and a sugar kinase domain annotated as a putative ROK-family regulator. Protein alignment shows a high amino acid sequence conservation of RokL6 in *Streptomyces* species (Fig. S1). Its genomic neighbors, SCO1446 and SCO1448, encode a putative integral membrane protein and a Major Facilitator Superfamily (MFS) transporter with unknown substrates, and the intergenic regions of *rokL6*-SCO1446 and *rokL6*-SCO1448 are 21 and 112 bp long,

respectively (Fig. 2A). There is significant gene synteny for the genomic region surrounding *rokL6* and its orthologues in *Streptomyces*. In particular, SCO1448 and its homologs, often lie divergently transcribed from the corresponding ROK regulators encoding genes (Fig. 2B). The *rokL6*-SCO1448 unit is also identified in many *Kitasatospora* species (Fig. S2).

Given the importance of ROK-family regulators in the control of sugar utilization (26) and the likelihood of the involvement of RokL6 in GlcN metabolism, we investigated its potential role in GlcN utilization by measuring the dry weights at different time points to compare the growth patterns of *S. coelicolor* M145 and its *rokL6* mutant in NMMP containing 1% GlcN as the sole carbon source. The mutant grew well in NMMP supplemented with either 1% glucose or with 1% GlcN (Fig. S3).

Transcriptome analysis of the *rokL6* mutant

To obtain further insights into the regulon of RokL6 and its relationship to GlcN metabolism, RNA-Seq analysis was performed using RNA extracted from *S. coelicolor* M145 and its *rokL6* mutant. For this, mycelia were grown on MM agar plates overlayed with cellophane discs, with either 1% (w/v) mannitol (Mann) or 1% (w/v) mannitol + 50 mM GlcN (GlcN) as the carbon sources. Biomass was harvested at two time points corresponding to vegetative growth (VEG) and sporulation (SPO). All samples were assessed as biological triplicates. In total 29 genes were significantly differentially expressed under at least one of the conditions analysed, using an adjusted *p*-value < 0.01 and a log2 fold change >2 or < -2 as threshold (Table S3). SCO1446 and SCO1448-SCO1450, which flank *rokL6,* were up-regulated in the *rokL6* mutant under all tested conditions (Fig. 3). In addition, SCO0476 (for an unknown ABC transport protein) was down-regulated at 24h. In the absence of GlcN, transcription of the *pstSCA* operon (SCO4140-4142), which is part of the PhoP regulon and related to the

transport of inorganic phosphate (55), was significantly up-regulated (> 4-fold), while SCO5338 (probable regulatory protein) and SCO5339 (probable plasmid transfer protein) were down-regulated in Δ*rokL6* during sporulation (Fig. 3A). In the presence of GlcN, the putative ABC transporter genes SCO3704-SCO3706 were up-regulated in Δ*rokL6* during sporulation in the presence of GlcN; transcription of genes in the biosynthetic gene cluster for carotenoid biosynthesis (56), including *crtE* (SCO0185), *crtI* (SCO0186), *crtB* (SCO0187), *crtY* (SCO0191), *litQ* (SCO0192) and the regulatory gene *litR* (SCO0193), were all strongly down-regulated in the *rokL6* mutant during vegetative growth (Fig. 3B). Indeed, compared to the wild-type M145, the production of carotenoids was significantly reduced in Δ*rokL6* in the presence of GlcN when plates were incubated in the light (Fig. S4), suggesting that RokL6 indeed plays a role in the control of carotenoid biosynthesis in *S. coelicolor*.

RokL6 specially binds to the intergenic region of *rokL6* and SCO1448

To identify direct targets of RokL6 *in vivo*, we performed Chromatin Immuno-Precipitation combined with sequencing (ChIP-Seq). For this, we constructed a strain expressing RokL6 with a $FLAG_3$ tag, as described in the Materials and Methods section. We used CRISPR-Cas9 technology to construct strain *S. coelicolor* M145-*rokL6*-FLAG, which has an engineered in-frame 3×FLAG epitope fused *in situ* and before the stop codon of *rokL6*. The functionality of RokL6-$FLAG_3$ was verified by introducing pCOM-FLAG into Δ*nagB*Δ*rokL6*. Indeed, while Δ*nagB*Δ*rokL6* mutants grow well on MM with mannitol and GlcN, Δ*nagB*Δ*rokL6*-FLAG expressing RokL6-$FLAG_3$ failed to grow (Fig. S5), showing that the RokL6-$FLAG_3$ was indeed expressed and active. ChIP-Seq analysis was performed with M145-*rokL6*-FLAG using cultures grown for 24 h and 48 h on MM with mannitol and MM with mannitol and GlcN. Under all conditions tested, only one major binding event was observed in all of the

samples, namely to the intergenic region of *rokL6* and SCO1448 (Fig. 4A). Binding of RokL6 to the intergenic region shared between *rokL6* and SCO1448 was further verified *in vitro* by electromobility shift assays (EMSAs). For this, C-terminally 6×His-tagged RokL6, RokL6-His_6, was expressed and purified from *E. coli* BL21(DE3). Compared to the probe for negative control, *hrdB* promoter (*hrdB*-P), which exhibited no retardation in the presence of RokL6, the result shows that RokL6 caused a strong retardation on the probe corresponding to the promoter region of *rokL6*-SCO1448 (SCO1448-P). Specifically, almost all SCO1448-P was bound when 1 μM RokL6-His_6 was added in the EMSA (Fig. 4B).

RokL6 binds to the inverted repeat *rokL6*-IR

Due to the high conservation in terms of both amino acid sequence and gene synteny of *rokL6* and SCO1448 with their orthologous, we reasoned that the orthologs of RokL6 may be autoregulators. To identify a putative RokL6 binding consensus, the intergenic DNA sequence of *S. coelicolor rokL6* and SCO1448, and 10 additional orthologous gene pairs from other streptomycetes (Table 1) were analysed for the presence of conserved motifs using MEME. This identified a highly conserved inverted repeat sequence of 23 nucleotides in all intergenic regions (Fig. 5A). The consensus of the motif was C(T)TATCAGG - 7 nt - CCTGATAG(A), which contains an inverted repeat designated as *rokL6*-IR, a primary candidate for the RokL6 binding site.

To verify if this is indeed a *bona fide* RokL6 binding site, EMSAs were performed using 60 bp probes. These probes contained either the intact *rokL6*-IR sequence (probe RokL6-BS) or mutant versions in which one or two regions of *rokL6*-IR were replaced by *Eco*RI or *Bam*HI restriction sites (probe RokL6-M1 to M3). Compared to RokL6-BS, which was bound at all tested concentrations (0.1, 0.2, and 0.5 μM) of RokL6-His_6, the binding signals of RokL6-His_6

to the mutated probes RokL6-M1 and RokL6-M2 was weakened, and to RokL6-M3 was fully abolished (Fig. 5B). Thes data show that the inverted repeat sequence *rokL6*-IR is indeed an essential part of the RokL6 binding site.

To determine if RokL6 has other binding sites on the *S. coelicolor* genome, the sequence of *rokL6*-IR was used to scan the *S. coelicolor* genome using PREDetector algorithm (50). In addition to the promoter regions of *rokL6* and SCO1448, one putative motif was identified with relative high score upstream of SCO0137 encoding a PTS EII with unknown substrate (Table S4). EMSAs showed that binding between RokL6 and the promoter of SCO0137 (SCO0137-P) *in vitro* was very weak (Fig. S6A). The putative PTS transporter EII genes SCO0137 and SCO0136 are co-expressed from a single transcriptional unit; to see if the operon would be the major GlcN transporter, a mutant was created in both the wild-type strain *S. coelicolor* M145 and in the *nagB* mutant. For this, the region from nt position +10 of SCO0137 to nt position + 1542 of SCO0136 was replaced by the apramycin resistance cassette *aac(3)IV* (see Materials and Methods). Deletion of SCO0136-SCO0137 in the *nagB* mutant did not relieve GlcN toxicity (Fig. S6B). This strongly suggests that SCO0136-SCO0137 are at least not solely responsible for GlcN transport in *S. coelicolor*.

Identification of the transcription start sites (TSS) for *rokL6* and SCO1448 and repression by RokL6

5’ rapid amplification of cDNA ends (5’ RACE) was applied to identify the promoters of both *rokL6* and SCO1448. Fragments of 5’ cDNA of *rokL6* and SCO1448 were PCR-amplified from the *S. coelicolor* genome and sequenced (Fig. S7). The TSS of *rokL6* was localized to a G located 67 nt upstream of the *rokL6* translation start codon (TSC), and the SCO1448 TSS was mapped to a G located 27 nt upstream of the SCO1448 TSC (Fig. 6A). The RokL6 binding site

rokL6-IR encompasses nt positions -7 to +14 relative to the *rokL6* TSS, which is immediately downstream of the putative -10 region of the *rokL6* promoter. Suggestively, the *rokL6*-IR is located exactly between the -10 and -35 sequences of the SCO1448 promoter. This places the RokL6 binding site in the ideal position to repress both genes at the same time. Binding of the repressor close to the -10 or -35 consensus boxes for the RNA polymerase sigma factor is common, as it interferes with the recognition, binding of RNA polymerase, and the formation of the transcriptional initiation complex (57). This suggests that RokL6 represses the transcription of both SCO1448 and *rokL6* by binding to the core promoter regions to prevent their transcription from proceeding properly.

To determine if this is indeed the case, promoter activity assays were performed using promoters P*rokL6* (*rokL6* promoter), P1448 (SCO1448 promoter), P*nagKA* (*nagKA* promoter) and P30, with eGFP as the reporter and cloned into the integrative vector pSET152. The resulting vectors pEGFP-*rokL6*, pEGFP-1448, pEGFP-*nagKA* and pEGFP-P30 were introduced into *S. coelicolor* M145 and Δ*rokL6*. The recombinant strains were grown on MM agar with 1% mannitol and analysed for eGFP expression levels by florescence microscopy and qPCR. When eGFP was expressed from either the *nagKA* promoter or the artificial promoter P30, fluorescence was unchanged between M145 and Δ*rokL6*. Conversely, when expressed from either P*rokL6* or P1448, eGFP levels were significantly higher in Δ*rokL6* as compared to the parental strain M145 (Fig. 6B). This result was confirmed by qPCR for the transcription of the gene for eGFP, with enhanced expression of eGFP in the *rokL6* mutant as compared to the parent, while again no significant differences in expression levels were observed for either P*nagKA* or P30. However, the transcript levels of the gene for eGFP from both P*rokL6* and P1448 were significantly up-regulated in Δ*rokL6* (Fig. 6C), suggesting that

RokL6 indeed represses the transcription of both SCO1448 and at the same time acts as an autoregulator.

Overexpression of transporter SCO1448 relieves GlcN toxicity in *nagB* mutants

The data above demonstrate that putative transporter protein SCO1448 is the primary target of RokL6. We therefore hypothesized that SCO1448 may function as an exporter of a toxic metabolic intermediate that accumulates in *nagB* mutants grown on media containing GlcN. Inactivation of the repressor gene *rokL6* results in enhanced expression of SCO1448, alleviating GlcN toxicity, presumably by exporting a toxic intermediate. If this is indeed the case, expressing SCO1448 from a RokL6-independent (constitutive) promoter should have the same effect as deleting *rokL6*. To test this, SCO1448 was placed under the control of the strong and constitutive P30 promoter (see Materials and Methods for details), and introduced into Δ*nagB* to obtain SCO1448 over-expression strain, Δ*nagB*SCO1448-O. As a control, we used empty plasmid pSET152, to obtain Δ*nagB*-E. Transcription levels of SCO1448 were measured, showing that in both the de-repressed Δ*nagB*Δ*rokL6* and the overexpressing Δ*nagB*SCO1448-O strains, SCO1448 was highly expressed (Fig. 7A). Importantly, RokL6-independent expression of SCO1448 fully alleviated toxicity of *nagB* mutants to GlcN, while Δ*nagB* or Δ*nagB* with the empty plasmid were still sensitive to GlcN (Fig. 7B).

Finally, we evaluated the viability of SCO1448 knock-out mutants in the presence of GlcN. For this, the coding regions of SCO1448, spanning nucleotides +6 to +1023 (relative to the transcriptional start site), were substituted with the apramycin resistance cassette *aac(3)IV*, in *S. coelicolor* M145, Δ*nagB*, SMG1 (Δ*nagB* with a suppressor mutation in *rokL6*), and Δ*nagB*Δ*rokL6*. Homologous recombination of the gene was achieved by introduction of

vector pKO-1448, which was constructed by cloning the resistance cassette between the upstream and downstream flanking regions of SCO1448 in the unstable multi-copy plasmid pWHM3. Correct recombination events were confirmed by resistance to apramycin and sensitivity to thiostrepton (for loss of the plasmid) and by PCR, thus obtaining SCO1448 knock-out mutants, ΔSCO1448, Δ*nagB*ΔSCO1448, SMG1ΔSCO1448, and Δ*nagB*Δ*rokL6*ΔSCO1448. As expected, when SCO1448 was deleted in suppressor mutant SMG1 or in Δ*nagB*Δ*rokL6*, neither strain could grow in the presence of GlcN (Fig. 7C). This again provides compelling evidence that SCO1448 is solely responsible for alleviating the toxicity of GlcN to *nagB* mutants. Taken together, our data show that RokL6 directly represses the expression of SCO1448, and that in turn, SCO1448 is responsible for alleviating GlcN toxicity to *nagB* mutants. It is likely that SCO1448 exports toxic metabolic intermediates derived from GlcN-6P that accumulates in *nagB* mutants of *S. coelicolor* when grown on GlcN.

DISCUSSION

The aminosugar *N*-acetylglucosamine (GlcNAc) is a preferred nutrient for *Streptomyces* and also acts as a signaling molecule for the nutritional status of the environment. While GlcNAc metabolism and transport in streptomycetes have been well studied, little is known about how GlcN is metabolized in *Streptomyces*. *S. coelicolor nagB* mutants, which cannot convert GlcN-6P into the glycolytic intermediate Fru-6P, fail to grow on either GlcNAc or GlcN, indicating that toxic intermediates are produced when GlcN-6P is not actively metabolized by NagB. We used this feature to select for suppressor mutants, whereby it is important to note that some *nagB* suppressors selected on GlcNAc fail to confer resistance to GlcN and *vice versa*. In this work we focused on the GlcN-specific gene *rokL6* (SCO1447), mutation of which relieves GlcN toxicity in *nagB* mutants.

RokL6 is a ROK-family regulator, and members of this family of regulators often play a role in the control of sugar metabolism. Systems-wide analysis using RNA-Seq, qPCR, ChIP-Seq and EMSAs showed that RokL6 (SCO1447) directly represses the transcription of the gene for SCO1448, which is annotated as an MFS sugar transporter. SCO1448 plays a key role in alleviating GlcN toxicity in the absence of NagB activity. Up-regulation of SCO1448 is sufficient to relieve GlcN toxicity to *S. coelicolor nagB* mutants, while conversely, deletion of SCO1448 in *S. coelicolor* Δ*nagB*Δ*rokL6* or the suppressor mutant SMG1 abolishes the acquired GlcN resistance (Fig. 7). Thus, the key to GlcN resistance lies in the expression of SCO1448. Still, a lot is unclear about the *rokL6*-SCO1448 gene pair. In particular, why would streptomycetes have a cryptic exporter to protect themselves from toxic intermediates related specifically to GlcN? The system is likely important, as its gene synteny and also (the location of) the RokL6 binding site are highly conserved in *Streptomyces* and its sister genus *Kitasatospora* (Fig. 2B and Table 1). The high conservation of the binding site predicts that expression of SCO1448 is repressed by RokL6 in many if not all streptomycetes. While the biological significance it is not yet understood, the proteins likely play an important role in preventing the accumulation of excess toxic intermediates under specific growth conditions in the natural environment. How the repression by RokL6 is relieved in the cell and what the possible ligands are that control its DNA binding, which likely facilitates the derepression of SCO1448, remains to be elucidated.

An important question is also what the exact nature is of the toxic molecule(s) that accumulate in *nagB* mutants, which are likely derived from GlcN-6P. Mutants that lack a functional NagA enzyme accumulate high levels of GlcNAc-6P, which is lethal in *E. coli* and *B. subtilis* (22, 23, 58). However, *S. coelicolor nagA* null mutants are able to grow in the presence of either GlcNAc or GlcN, and deletion of *nagA* from *nagB* null mutants of *S.*

coelicolor also alleviate the toxicity of either aminosugar (24). However, there are no metabolic routes that point at a key role for NagA in GlcN metabolism. Why then would mutation of *nagA* prevent toxicity of not only GlcNAc but also GlcN in *nagB* mutants? This again shows that there are still significant gaps in our understanding of aminosugar metabolism in *Streptomyces*. This is in fact quite surprising for such an important central metabolic pathway.

ChIP-Seq and EMSA assays demonstrated that RokL6 binds directly to the palindromic *rokL6*-IR identified from the intergenic region of *rokL6* and SCO1448, with the sequence 5' -C(T)TATCAGG - 7 nt - CCTGATAG(A)- 3'. Furthermore, the precise transcription start sites for *rokL6* and SCO1448 were identified by 5' RACE, showing that the two genes are transcribed from overlapping promoters. RokL6 strategically binds to a site that is located precisely in between the -35 and -10 boxes for SCO1448 and downstream of the -10 box for *rokL6*, allowing RokL6 to inhibit the transcription of both genes at the same time. The transcriptional repression of SCO1448 and autoregulation of *rokL6* by RokL6 was further demonstrated by promoter activity assays and qPCR (Fig. 6), showing that RokL6 indeed inhibits the transcription of both genes.

The RokL6 binding site is distinct from operators characterized for ROK-family regulators in *e.g. E. coli* and Firmicutes. The operator consensus sequences of NagC and Mlc in *E. coli* or XylR in firmicutes are typically composed of two A/T-rich inverted repeats separated by a spacer of 5-9 bp (19, 59, 60). The binding consensus sequences of RokB from *S. coelicolor* and RokA from *Streptococcus pneumoniae* are also enriched with T and A at the 5'-end and 3'-end (61, 62), similar to CysR from *Corynebacterium glutamicum* (63). The binding target of CsnR from *S. lividans* shares some similarity with that of RokL6, containing the sequence 5' -AGG - 7 nt - CCT- 3' in the binding consensus. In contrast, the binding

consensus of Rok7B7 of *S. avermitilis* is 5′ -TTKAMKHSTTSAV- 3′ and unrelated to that of RoL6 (19, 26).

ChIP-seq experiments identified a single binding site in all samples. Using that binding consensus as input, scanning the *S. coelicolor* genome using PREDetector revealed one additional sequence with similarity to the RokL6 consensus, namely upstream of the SCO0137-SCO0136 operon that encodes PTS transporter EIIC enzymes. Its control by RokL6 and the fact that in *E. coli* and *B. subtilis*, GlcN is transported via the PTS (64-66), suggested a possible role for the SCO0137-SCO0136 operon in GlcN transport. We tested whether inactivation of the operon would affect GlcN toxicity in *nagB* mutants, but this as not the case (Fig. S6B). Therefore, PTS transporter SCO0136-SCO0137 is at least not the only transporter for GlcN uptake in *S. coelicolor*, and more studies are required to understand how GlcN is internalized in streptomycetes.

In terms of indirect effects of the deletion of *rokL6,* besides SCO1448 also the adjacent SCO1446 and SCO1448-SCO1450 were upregulated in *rokL6* mutants. Other genes whose transcription was affected were those for transporters SCO0476, SCO3704-SCO3706 and SCO4140-SCO4142, as well as for genes of the carotenoid biosynthetic gene cluster (BGC). Upregulation of the latter BGC was validated by enhanced pigmentation of mycelia grown in the light (Fig. S4). However, our experiments strongly suggest that the intergenic region between *rokL6* and SCO1448 is the primary binding site for RokL6, and the other genes whose transcription was affected in *rokL6* mutants are likely controlled indirectly.

Our current understanding of aminosugar metabolism and transport in *Streptomyces* is shown schematically in Fig. 8, including possible functions for RokL6 and SCO1448. GlcN-6P is derived either from the internalization of GlcN or the deacetylation of GlcNAc-6P. High accumulation of GlcN-6P and/or their metabolic derivatives is lethal to *S. coelicolor*, in line

with observations in *E. coli* and *B. subtilis*. The MFS transporter SCO1448 likely serves to facilitate the export of toxic intermediate(s), and in turn, the transcription of SCO1448 is repressed by RokL6 (Fig. 8). Constitutive expression of SCO1448 does not relieve the toxicity of GlcNAc, suggesting that GlcNAc and GlcN toxicity are not caused by the same molecule(s).

Taken together, this study characterizes the function of the ROK-family regulator RokL6, including its regulons, binding sites and its roles in the relief of GlcN toxicity in *S. coelicolor*. These findings shed new light on aminosugar sensitivity and on the control of aminosugar metabolism in *Streptomyces*, which plays a central role in their life cycle.

ACKNOWLEDGMENTS

We thank E. de Waal for technical assistance. This work was supported by a fellowship from the Chinese Scholarship Council (CSC) to C. Li.

Conflict of interest statement

The authors have no conflicts of interest to declare.

REFERENCES

1. Berdy J. 2005. Bioactive microbial metabolites. J Antibiot 58:1-26.
2. Hopwood DA. 2007. *Streptomyces* in nature and medicine: the antibiotic makers. Oxford University Press.
3. Barka EA, Vatsa P, Sanchez L, Gaveau-Vaillant N, Jacquard C, Klenk H-P, Clément C, Ouhdouch Y, van Wezel GP. 2016. Taxonomy, physiology, and natural products of Actinobacteria. Microbiol Mol Biol Rev 80:1-43.
4. Bibb MJ. 2005. Regulation of secondary metabolism in streptomycetes. Curr Opin Microbiol 8:208-15.
5. van der Heul HU, Bilyk BL, McDowall KJ, Seipke RF, van Wezel GP. 2018. Regulation of antibiotic production in Actinobacteria: new perspectives from the post-genomic era. Nat Prod Rep 35:575-604.
6. Flärdh K, Buttner MJ. 2009. *Streptomyces* morphogenetics: dissecting differentiation in a filamentous bacterium. Nat Rev Microbiol 7:36-49.
7. Manteca A, Fernandez M, Sanchez J. 2005. Mycelium development in *Streptomyces antibioticus* ATCC11891 occurs in an orderly pattern which determines multiphase growth curves. BMC microbiology 5:51.
8. Tenconi E, Traxler MF, Hoebreck C, van Wezel GP, Rigali S. 2018. Production of Prodiginines Is Part of a Programmed Cell Death Process in *Streptomyces coelicolor*. Front Microbiol 9:1742.
9. Borisova M, Gaupp R, Duckworth A, Schneider A, Dalügge D, Mühleck M, Deubel D, Unsleber S, Yu W, Muth G. 2016. Peptidoglycan recycling in Gram-positive bacteria is crucial for survival in stationary phase. MBio 7:e00923-16.
10. Nothaft H, Dresel D, Willimek A, Mahr K, Niederweis M, Titgemeyer F. 2003. The phosphotransferase system of *Streptomyces coelicolor* is biased for N-acetylglucosamine metabolism. J Bacteriol 185:7019-7023.
11. Nothaft H, Rigali S, Boomsma B, Swiatek M, McDowall KJ, Van Wezel GP, Titgemeyer F. 2010. The permease gene *nagE2* is the key to N-acetylglucosamine sensing and utilization in *Streptomyces coelicolor* and is subject to multi-level control. Mol Microbiol 75:1133-1144.
12. Świątek MA, Tenconi E, Rigali S, van Wezel GP. 2012. Functional analysis of the N-acetylglucosamine metabolic genes of *Streptomyces coelicolor* and role in control of development and antibiotic production. J Bacteriol 194:1136-1144.
13. Urem M, Świątek-Połatyńska MA, Rigali S, van Wezel GP. 2016. Intertwining nutrient-sensory networks and the control of antibiotic production in *Streptomyces*. Mol Microbiol 102:183-195.
14. Rigali S, Nothaft H, Noens EE, Schlicht M, Colson S, Müller M, Joris B, Koerten HK, Hopwood DA, Titgemeyer F. 2006. The sugar phosphotransferase system of *Streptomyces coelicolor* is regulated by the GntR-family regulator DasR and links N-acetylglucosamine metabolism to the control of development. Mol Microbiol 61:1237-1251.
15. Rigali S, Titgemeyer F, Barends S, Mulder S, Thomae AW, Hopwood DA, Van Wezel GP. 2008. Feast or famine: the global regulator DasR links nutrient stress to antibiotic production by *Streptomyces*. EMBO Rep 9:670-675.
16. Świątek-Połatyńska MA, Bucca G, Laing E, Gubbens J, Titgemeyer F, Smith CP, Rigali S, van Wezel GP. 2015. Genome-wide analysis of *in vivo* binding of the master regulator DasR in *Streptomyces coelicolor* identifies novel non-canonical targets. PLoS One 10:e0122479.
17. Craig M, Lambert S, Jourdan S, Tenconi E, Colson S, Maciejewska M, Ongena M, Martin JF, van Wezel G, Rigali S. 2012. Unsuspected control of siderophore production by N-acetylglucosamine in streptomycetes. Environ Microbiol Rep 4:512-521.
18. Rigali S, Anderssen S, Naômé A, van Wezel GP. 2018. Cracking the regulatory code of biosynthetic gene clusters as a strategy for natural product discovery. Biochem Pharmacol 153:24-34.

19. Dubeau M-P, Poulin-Laprade D, Ghinet MG, Brzezinski R. 2011. Properties of CsnR, the transcriptional repressor of the chitosanase gene, *csnA*, of *Streptomyces lividans*. J Bacteriol 193:2441-2450.
20. Viens P, Dubeau M-P, Kimura A, Desaki Y, Shinya T, Shibuya N, Saito A, Brzezinski R. 2015. Uptake of chitosan-derived D-glucosamine oligosaccharides in *Streptomyces coelicolor* A3 (2). FEMS Microbiol Lett 362.
21. Titgemeyer F, Reizer J, Reizer A, Saier Jr MH. 1994. Evolutionary relationships between sugar kinases and transcriptional repressors in bacteria. Microbiology 140:2349-2354.
22. Plumbridge J. 2009. An alternative route for recycling of N-acetylglucosamine from peptidoglycan involves the N-acetylglucosamine phosphotransferase system in *Escherichia coli*. J Bacteriol 191:5641-5647.
23. Plumbridge J. 2015. Regulation of the utilization of amino sugars by *Escherichia coli* and *Bacillus subtilis*: same genes, different control. Microb Physiol 25:154-167.
24. Świątek MA, Urem M, Tenconi E, Rigali S, van Wezel GP. 2012. Engineering of N-acetylglucosamine metabolism for improved antibiotic production in *Streptomyces coelicolor* A3 (2) and an unsuspected role of NagA in glucosamine metabolism. Bioengineered 3:280-285.
25. Świątek MA, Gubbens J, Bucca G, Song E, Yang Y-H, Laing E, Kim B-G, Smith CP, van Wezel GP. 2013. The ROK family regulator Rok7B7 pleiotropically affects xylose utilization, carbon catabolite repression, and antibiotic production in *Streptomyces coelicolor*. J Bacteriol 195:1236-1248.
26. Lu X, Liu X, Chen Z, Li J, van Wezel GP, Chen W, Wen Y. 2020. The ROK-family regulator Rok7B7 directly controls carbon catabolite repression, antibiotic biosynthesis, and morphological development in *Streptomyces avermitilis*. Environ Microbiol 22:5090-5108.
27. Sambrook J, Fritsch EF, Maniatis T. 1989. Molecular cloning: a laboratory manual. Cold spring harbor laboratory press.
28. MacNeil DJ, Gewain KM, Ruby CL, Dezeny G, Gibbons PH, MacNeil T. 1992. Analysis of *Streptomyces avermitilis* genes required for avermectin biosynthesis utilizing a novel integration vector. Gene 111:61-68.
29. Hoskisson PA, van Wezel GP. 2019. *Streptomyces coelicolor*. Trends Microbiol 27:468-469.
30. Swiatek MA. 2012. Global control of development and antibiotic production by nutrient-responsive signalling pathways in *Streptomyces*Leiden University.
31. Kieser T, Bibb MJ, Buttner MJ, Chater KF, Hopwood DA. 2000. Practical *Streptomyces* genetics, vol 291. John Innes Foundation Norwich.
32. Vara J, Lewandowska-Skarbek M, Wang Y-G, Donadio S, Hutchinson C. 1989. Cloning of genes governing the deoxysugar portion of the erythromycin biosynthesis pathway in *Saccharopolyspora erythraea* (*Streptomyces erythreus*). J Bacteriol 171:5872-5881.
33. Zhang L, Willemse J, Hoskisson PA, van Wezel GP. 2018. Sporulation-specific cell division defects in *ylmE* mutants of *Streptomyces coelicolor* are rescued by additional deletion of *ylmD*. Sci Rep 8:1-13.
34. Khodakaramian G, Lissenden S, Gust B, Moir L, Hoskisson PA, Chater KF, Smith MC. 2006. Expression of Cre recombinase during transient phage infection permits efficient marker removal in *Streptomyces*. Nucleic Acids Res 34:e20-e20.
35. Fedoryshyn M, Welle E, Bechthold A, Luzhetskyy A. 2008. Functional expression of the Cre recombinase in actinomycetes. Appl Microbiol Biotechnol 78:1065-1070.
36. Bierman M, Logan R, O'brien K, Seno E, Rao RN, Schoner B. 1992. Plasmid cloning vectors for the conjugal transfer of DNA from *Escherichia coli* to *Streptomyces* spp. Gene 116:43-49.
37. Bai C, Zhang Y, Zhao X, Hu Y, Xiang S, Miao J, Lou C, Zhang L. 2015. Exploiting a precise design of universal synthetic modular regulatory elements to unlock the microbial natural products in *Streptomyces*. Proc Natl Acad Sci U S A 112:12181-12186.

38. Cobb RE, Wang Y, Zhao H. 2015. High-efficiency multiplex genome editing of *Streptomyces* species using an engineered CRISPR/Cas system. ACS Synth Biol 4:723-728.
39. Du C, Willemse J, Erkelens AM, Carrion VJ, Dame RT, van Wezel GP. 2022. System-wide analysis of the GATC-binding nucleoid-associated protein Gbn and its impact on *Streptomyces* development. mSystems 7:e00061-22.
40. Guo J, Zhang X, Lu X, Liu W, Chen Z, Li J, Deng L, Wen Y. 2018. SAV4189, a MarR-family regulator in *Streptomyces avermitilis*, activates avermectin biosynthesis. Front Microbiol 9:1358.
41. Chen S, Zhou Y, Chen Y, Gu J. 2018. fastp: an ultra-fast all-in-one FASTQ preprocessor. Bioinformatics 34:i884-i890.
42. Langmead B, Salzberg SL. 2012. Fast gapped-read alignment with Bowtie 2. Nat Methods 9:357-359.
43. Liao Y, Smyth GK, Shi W. 2014. featureCounts: an efficient general purpose program for assigning sequence reads to genomic features. Bioinformatics 30:923-930.
44. Love MI, Huber W, Anders S. 2014. Moderated estimation of fold change and dispersion for RNA-seq data with DESeq2. Genome Biol 15:1-21.
45. Zhu A, Ibrahim JG, Love MI. 2019. Heavy-tailed prior distributions for sequence count data: removing the noise and preserving large differences. Bioinformatics 35:2084-2092.
46. Vandesompele J, De Preter K, Pattyn F, Poppe B, Van Roy N, De Paepe A, Speleman F. 2002. Accurate normalization of real-time quantitative RT-PCR data by geometric averaging of multiple internal control genes. Genome Biol 3:1-12.
47. Celler K, Koning RI, Willemse J, Koster AJ, van Wezel GP. 2016. Cross-membranes orchestrate compartmentalization and morphogenesis in *Streptomyces*. Nat Commun 7:11836.
48. Oberto J. 2013. SyntTax: a web server linking synteny to prokaryotic taxonomy. BMC Bioinf 14:1-10.
49. Crooks GE, Hon G, Chandonia J-M, Brenner SE. 2004. WebLogo: a sequence logo generator. Genome Res 14:1188-1190.
50. Hiard S, Marée R, Colson S, Hoskisson PA, Titgemeyer F, van Wezel GP, Joris B, Wehenkel L, Rigali S. 2007. PREDetector: a new tool to identify regulatory elements in bacterial genomes. Biochem Biophys Res Commun 357:861-864.
51. Bailey TL, Boden M, Buske FA, Frith M, Grant CE, Clementi L, Ren J, Li WW, Noble WS. 2009. MEME SUITE: tools for motif discovery and searching. Nucleic Acids Res 37:W202-W208.
52. Barrett T, Wilhite SE, Ledoux P, Evangelista C, Kim IF, Tomashevsky M, Marshall KA, Phillippy KH, Sherman PM, Holko M. 2012. NCBI GEO: archive for functional genomics data sets—update. Nucleic Acids Res 41:D991-D995.
53. Urem M. 2017. Signalling pathways that control development and antibiotic production in *Streptomyces*Leiden University.
54. Redenbach M, Kieser HM, Denapaite D, Eichner A, Cullum J, Kinashi H, Hopwood D. 1996. A set of ordered cosmids and a detailed genetic and physical map for the 8 Mb *Streptomyces coelicolor* A3 (2) chromosome. Mol Microbiol 21:77-96.
55. Martín JF, Liras P. 2021. Molecular mechanisms of phosphate sensing, transport and signalling in *Streptomyces* and related actinobacteria. Int J Mol Sci 22:1129.
56. Takano H, Obitsu S, Beppu T, Ueda K. 2005. Light-induced carotenogenesis in *Streptomyces coelicolor* A3 (2): identification of an extracytoplasmic function sigma factor that directs photodependent transcription of the carotenoid biosynthesis gene cluster. J Bacteriol 187:1825-1832.
57. Ruff EF, Record Jr MT, Artsimovitch I. 2015. Initial events in bacterial transcription initiation. Biomolecules 5:1035-1062.
58. White R. 1968. Control of amino sugar metabolism in *Escherichia coli* and isolation of mutants unable to degrade amino sugars. Biochem J 106:847-858.

59. El Qaidi S, Plumbridge J. 2008. Switching control of expression of *ptsG* from the Mlc regulon to the NagC regulon. J Bacteriol 190:4677-4686.
60. Gu Y, Ding Y, Ren C, Sun Z, Rodionov DA, Zhang W, Yang S, Yang C, Jiang W. 2010. Reconstruction of xylose utilization pathway and regulons in Firmicutes. BMC Genom 11:1-14.
61. Shafeeq S, Kloosterman TG, Rajendran V, Kuipers OP. 2012. Characterization of the ROK-family transcriptional regulator RokA of *Streptococcus pneumoniae* D39. Microbiology 158:2917-2926.
62. Bekiesch P, Forchhammer K, Apel AK. 2016. Characterization of DNA binding sites of RokB, a ROK-family regulator from *Streptomyces coelicolor* reveals the RokB regulon. PLoS One 11:e0153249.
63. Rückert C, Milse J, Albersmeier A, Koch DJ, Pühler A, Kalinowski J. 2008. The dual transcriptional regulator CysR in *Corynebacterium glutamicum* ATCC 13032 controls a subset of genes of the McbR regulon in response to the availability of sulphide acceptor molecules. BMC Genom 9:1-18.
64. Plumbridge J. 2000. A mutation which affects both the specificity of PtsG sugar transport and the regulation of *ptsG* expression by Mlc in *Escherichia coli*. Microbiology 146:2655-2663.
65. Zeppenfeld T, Larisch C, Lengeler JW, Jahreis K. 2000. Glucose transporter mutants of *Escherichia coli* K-12 with changes in substrate recognition of $IICB^{Glc}$ and induction behavior of the *ptsG* gene. J Bacteriol 182:4443-4452.
66. Gaugué I, Oberto J, Putzer H, Plumbridge J. 2013. The use of amino sugars by *Bacillus subtilis*: presence of a unique operon for the catabolism of glucosamine. PLoS One 8:e63025.

Table 1. Alignment of palindromic sequences found upstream of genes encoding RokL6 and its orthologs in streptomycetes

Microorganism	Gene name	Pos #	Sequence*
S.coelicolor	*rokL6*	-64	cgtaaactatcagggagcctgcctgatagatagtggatta
S.lividans	SLIV_30530	-64	cgtaaactatcagggagcctgcctgatagatagtggatta
*Streptomyces CCM*_MD2014	NI25_31970	-65	cgtaaactatcagggagcctgcctgatagatagtgcatta
S. ambofaciens	SAM40697_1335	-64	cgtaaactatcaggaaccctgcctgatagatagggatat
S. pactum	B1H29_30360	-65	cgtaaactatcaggaaccctgcctgatagataggcgatta
S. parvulus	SPA_05455	-65	cgtaaactatcagggaccctgcctgatagatagtggatta
S. aquilus	EJC51_09795	-51	cgtaaactatcagggaccctgcctgatagatagagcgtca
S. chromofuscus	IPT68_06320	-55	ggtaaattatcagggaccctgcctgatagatagagggcgt
S. cacaoi subsp. asoensis	G9272_09180	-74	cgtaaactatcaggaaccctgcctgataaatagaggccga
S. venezuelae ATCC 21113	DEJ44_04995	-64	ggtaaactatcaggaaccctgcctgataaatagaccgcag
S. cadmiisoli	DN051_31430	-72	ggtaaactatcaggaaccctgcctgatagatagggaccc

Position, distance in bp from the central nucleotide of the identified conserved sequence (shown in red) to the start codon of the associated gene.

* Bases conserved in palindromic sequences are shown in blue.

FIGURE LEGENDS

Figure 1. Sensitivity of *S. coelicolor* mutants to GlcN and GlcNAc. Spores (10^5 CFU) of *S. coelicolor* M145 or its mutant derivatives were streaked onto minimal medium (MM) with either 1% (w/v) mannitol (Mann), 5 mM *N*-acetylglucosamine (GlcNAc) or 5 mM glucosamine (GlcN) and grown for 72 h at 30˚C. Strains were *S. coelicolor* M145 (M145), its mutant derivatives Δ*nagB*, Δ*rokL6*, suppressor mutant SMG1, Δ*nagB*Δ*rokL6*, and the Δ*nagB*Δ*rokL6* mutant harboring either pCOM-*rokL6* (Δ*nagB*Δ*rokL6*-C) or empty vector pSET152 (Δ*nagB*Δ*rokL6*-E). Both top and bottom view are shown. Note that all strains without the gene *nagB* are sensitive to GlcNAc, while all strains lacking *rokL6* are resistant to GlcN.

Figure 2. Genetic organization and gene synteny around *rokL6*. (A) Genetic organization of the genomic region around *rokL*6. All open reading frames (ORFs) are depicted by solid arrows with their predicted gene products shown underneath; (B) Gene synteny of the region around *rokL6* in selected *Streptomyces* species. Synteny analysis was performed by Synttax (scores are given). Homologous genes are presented in the same colors. Homologs of *rokL6* and its neighbor SCO1448 are indicated in the dashed red box.

Figure 3. Heat maps of genes differentially expressed between the *rokL6* mutant and its parent *S. coelicolor* M145. Transcription patterns (expressed as log2 fold changes Δ*rokL6*/wild-type) are presented for genes differentially expressed when grown on MM with mannitol (A) or on MM with mannitol and GlcN (B). Only genes with an adjusted *p*-value less than 0.01 are shown. Navy, down-regulated (log2 fold change < -2) and brick red, up-

regulated (log2 fold change > 2) in the *rokL6* mutant; intermediate log2 fold changes represented in white. Genes significantly differentially expressed under all growth conditions are highlighted with red boxes.

Figure 4. Identification of RokL6 binding sites *in vivo* and *in vitro*. (A) Enrichment peaks of RokL6 by ChIP-Seq. Red line, ChIP sample; green line, input chromosomal DNA used as a negative control. Genes flanking the peak summits are indicated. Numbers on the *X*-axis indicate genomic positions. Samples were collected on mannitol (Mann) and mannitol with GlcN (GlcN) at two time points, vegetative phase (VEG) and sporulation phase (SPO). (B) EMSAs to establish direct binding in vitro. The binding of RokL6 to the intergenic sequence between *rokL6* and SCO1448 (SCO1448-P) was tested by EMSAs, with the *hrdB* promoter (*hrdB*-P) sequence as the negative control. Concentrations given in µM.

Figure 5. Identification of the RokL6 binding motif. (A) Sequence Logo representation of consensus sequence of RokL6 binding sites (analyzed by WebLogo). (B) RokL6 binding sites confirmation by EMSA. EMSAs of RokL6-His_6 with four probe sequences (RokL6-BS, RokL6-M1, RokL6-M2, RokL6-M3) were tested. The palindromic sequences (*rokL6*-IR) in Probe RokL6-BS are indicated by arrows. For each probe tested, the concentrations of RokL6-His_6 were 0.1, 0.2, and 0.5 µM.

Figure 6. RokL6 acts as transcriptional repressor of SCO1448 and as auto-repressor. (A) Nucleotide sequences of *rokL6* and SCO1448 promoter region and RokL6-binding site. Number, distance (nt) from the respective translation start codon (TSC); bent arrows, transcription start sites (TSS); boxes, start codons; grey shading, predicted -10 or -35 boxes

based on 5'RACE (Fig. S7); underlined, RokL6 binding site; straight arrow, direction of transcription. (B) Fluorescence intensity of eGFP measured based on confocal fluorescence micrographs. Mycelia of the strains transformed by eGFP with different promoters were imaged using confocal microscopy. Strains analysed as indicated: 1, M145-P*rokL6;* 2, M145-P1448; 3, M145-P*nagKA*; 4, M145-P30; 5, Δ*rokL6*-P*rokL6*; 6, Δ*rokL6*-P1448; 7, Δ*rokL6*-P*nagKA*; 8, Δ*rokL6*-P30. (C) Relative transcription levels of eGFP. Transcription levels of for eGFP gene expressed from different promoters (P*rokL6*, P1448, P*nagKA* and P30) in M145 and Δ*rokL6* were measured by qPCR analysis. Relative transcription levels were normalized to the transcription level of the gene for eGFP with P*rokL6* in M145, which was set as 1. Data were calculated from triplicate biological experiments and presented as mean ± SD (* $P < 0.05$).

Figure 7. Constitutive expression of SCO1448 relieves toxicity of *nagB* mutants to GlcN. (A) SCO1448 transcription levels analyzed by qPCR of the strains as follows, Δ*nagB*, Δ*nagB*Δ*rokL6*, Δ*nagB* with overexpressed SCO1448 (Δ*nagB*SCO1448-O), and Δ*nagB* complemented with empty pSET152 (Δ*nagB*-E). qPCR data were calculated from three independent experiments and presented as mean ± SD (* $P < 0.05$). (B) Growth of Δ*nagB*SCO1448-O on MM with GlcN(Ac). Spores of Δ*nagB*, Δ*nagB*Δ*rokL6*, Δ*nagB*SCO1448-O and Δ*nagB*-E, as indicated on the top, were spotted on MM with mannitol (Mann), MM with 1% mannitol and 5 mM GlcN (GlcN), and MM with 1% mannitol and 5 mM GlcNAc (GlcNAc) to determine their growth. (C) Growth of SCO1448 knock-out strains on GlcN. For media see (B).

Figure 8. Model for aminosugar metabolism and the roles of RokL6 and SCO1448 in *S. coelicolor*. Metabolism of GlcNAc is well understood in *S. coelicolor*. GlcN-6P is an allosteric inhibitor of the global repressor DasR, which represses the biosynthesis of antibiotics. Based on our data, we propose that toxic substances are formed from GlcN metabolism, in particular in *nagB* mutants; these are likely derived from GlcN-6P or its derivatives, and are exported by the MFS transporter SCO1448. We show that this transporter is transcriptionally repressed by the ROK-family regulator RokL6, and that expression of SCO1448 relieves GlcN toxicity. Metabolic routes are presented by black arrows with the enzymes as indicated/unknown routes by dotted arrows. Unknown transporters and enzymes are indicated by question marks. Note that toxic intermediates arising from GlcNAc are not relieved by SCO1448 and hence require at least in part another metabolic route. For details, see the main text. For abbreviations not mentioned in the text: Glc, glucose; Glc-6P, glucose-6-phosphate; GlcP, glucose permease, Glk, glucokinase; Pgi, glucose-6-phosphate isomerase; Glms, glucosamine-fructose-6-phosphate aminotransferase; CoA-Ac, Acetyl Coenzyme A; Act, actinorhodin; Red, prodiginines; Cda, calcium-dependent antibiotic; Cpk, cryptic polyketide.

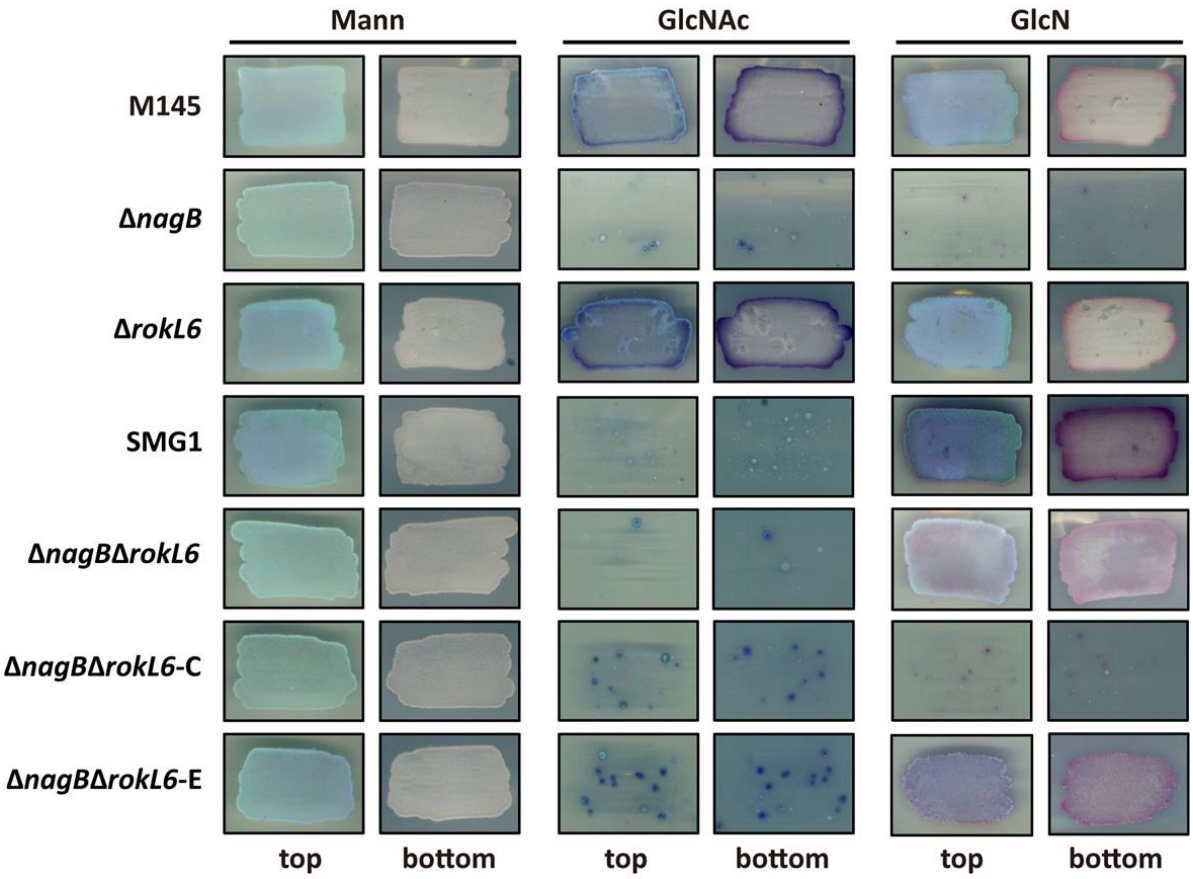
Mann
GlcNAc
GlcN
M145
ΔnagB
ΔrokL6
SMG1
ΔnagBΔrokL6
ΔnagBΔrokL6-C
ΔnagBΔrokL6-E
top
bottom
top
bottom
top
bottom

Figure 1

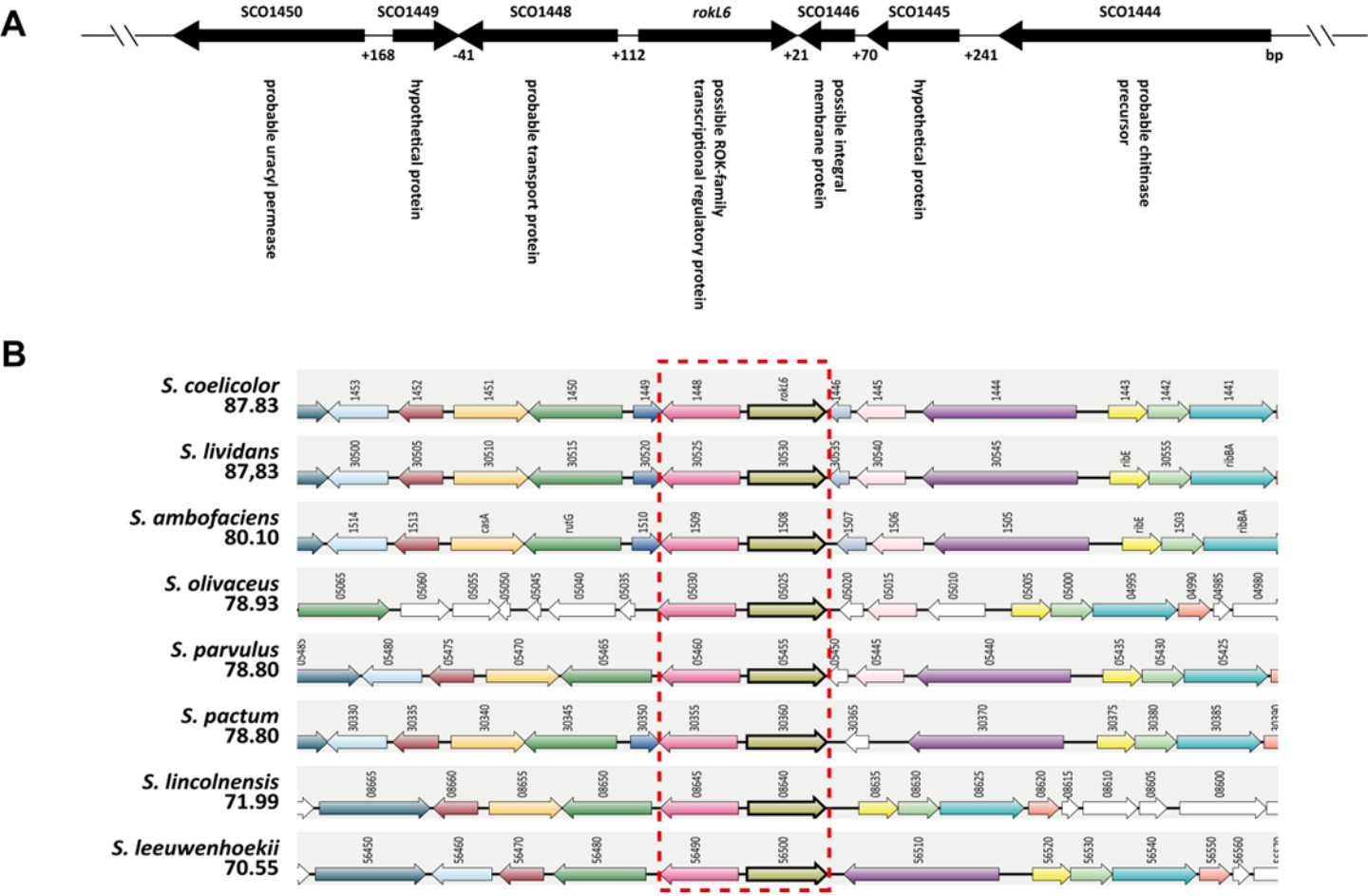
A
SCO1450
SCO1449
SCO1448
rokL6
SCO1446
SCO1445
SCO1444
+168
-41
+112
+21
+70
+241
bp
probable uracyl permease
hypothetical protein
probable transport protein
possible ROK-family transcriptional regulatory protein
possible integral membrane protein
hypothetical protein
probable chitinase precursor
B
S. coelicolor 87.83
S. lividans 87,83
S. ambofaciens 80.10
S. olivaceus 78.93
S. parvulus 78.80
S. pactum 78.80
S. lincolnensis 71.99
S. leeuwenhoekii 70.55

Figure 2

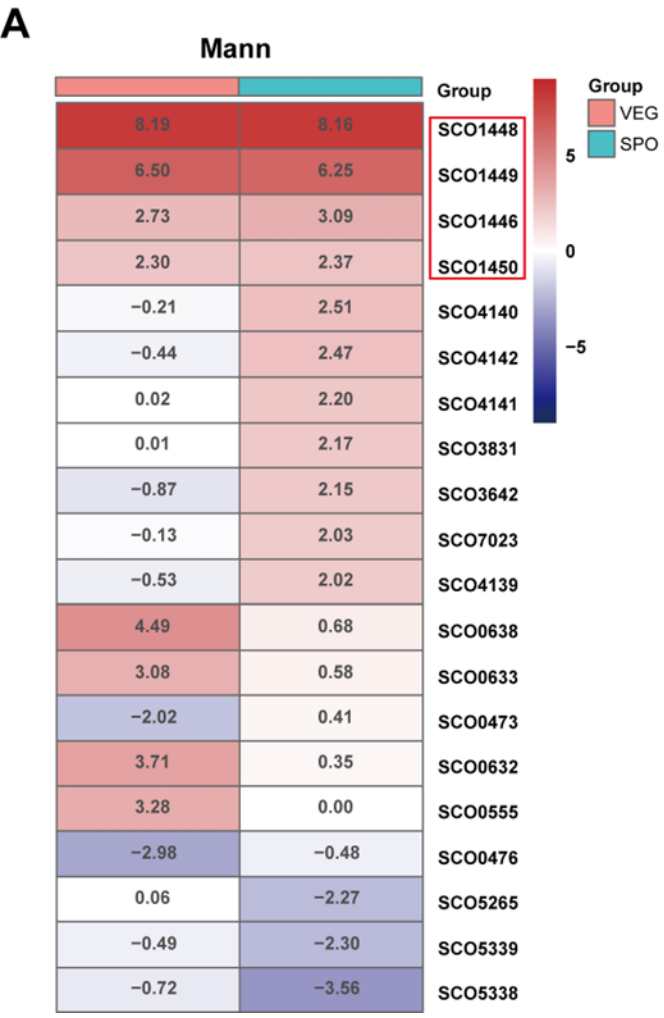
A
Mann
Group
VEG
SPO
5
0
−5
8.19 8.16 SCO1448
6.50 6.25 SCO1449
2.73 3.09 SCO1446
2.30 2.37 SCO1450
−0.21 2.51 SCO4140
−0.44 2.47 SCO4142
0.02 2.20 SCO4141
0.01 2.17 SCO3831
−0.87 2.15 SCO3642
−0.13 2.03 SCO7023
−0.53 2.02 SCO4139
4.49 0.68 SCO0638
3.08 0.58 SCO0633
−2.02 0.41 SCO0473
3.71 0.35 SCO0632
3.28 0.00 SCO0555
−2.98 −0.48 SCO0476
0.06 −2.27 SCO5265
−0.49 −2.30 SCO5339
−0.72 −3.56 SCO5338

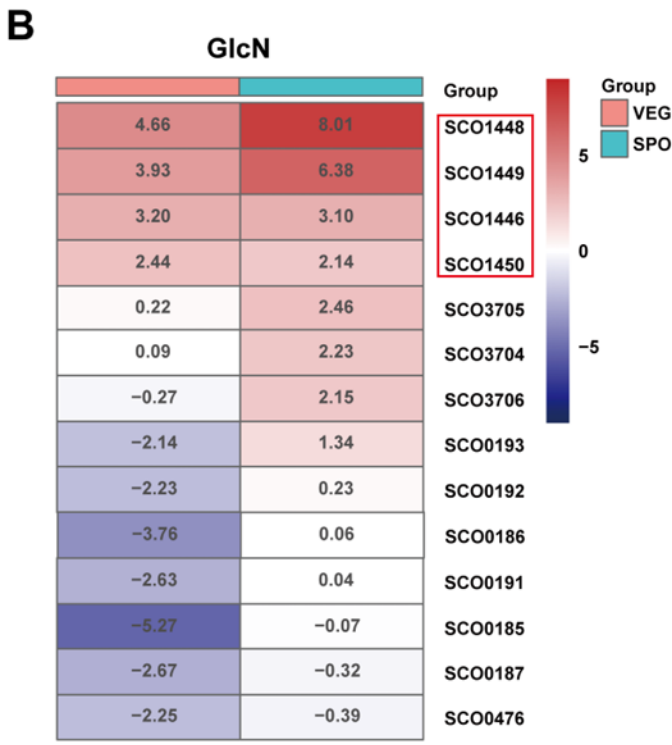
B
GlcN
Group
VEG
SPO
5
0
−5
4.66 8.01 SCO1448
3.93 6.38 SCO1449
3.20 3.10 SCO1446
2.44 2.14 SCO1450
0.22 2.46 SCO3705
0.09 2.23 SCO3704
−0.27 2.15 SCO3706
−2.14 1.34 SCO0193
−2.23 0.23 SCO0192
−3.76 0.06 SCO0186
−2.63 0.04 SCO0191
−5.27 −0.07 SCO0185
−2.67 −0.32 SCO0187
−2.25 −0.39 SCO0476

Figure 3

A

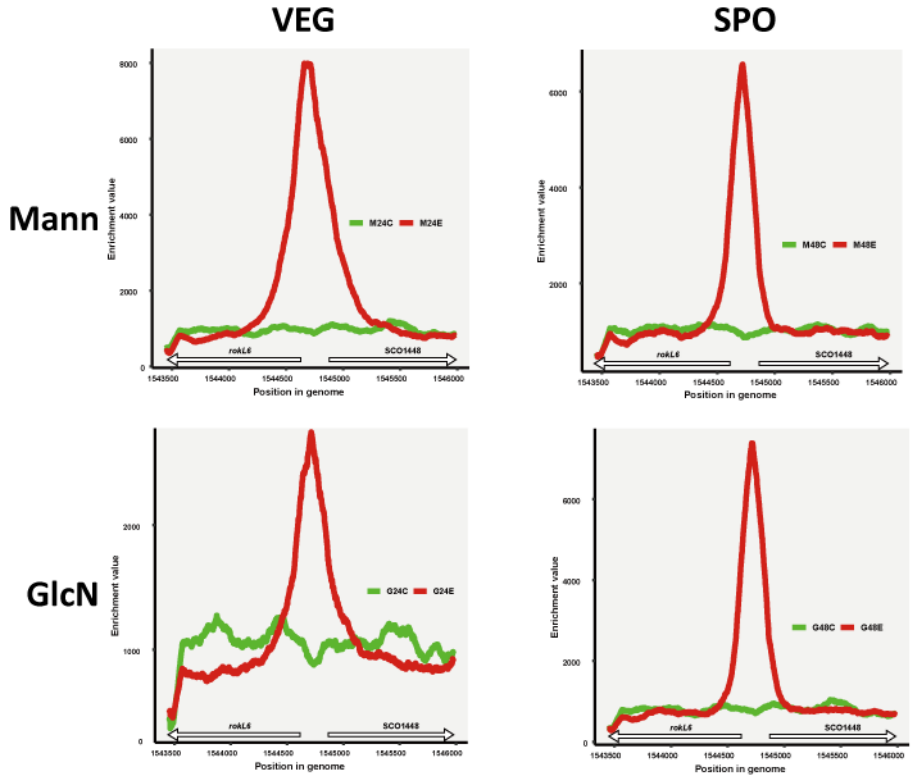
VEG
SPO
Mann
GlcN
Enrichment value
Position in genome
M24C
M24E
M48C
M48E
G24C
G24E
G48C
G48E
rokL6
SCO1448

B

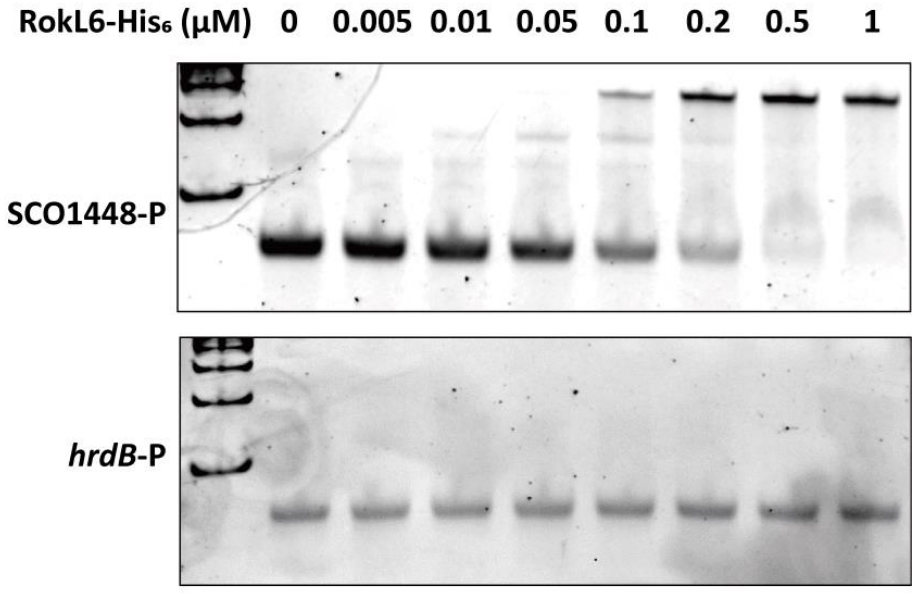
RokL6-His6 (μM) 0 0.005 0.01 0.05 0.1 0.2 0.5 1
SCO1448-P
hrdB-P

Figure 4

A

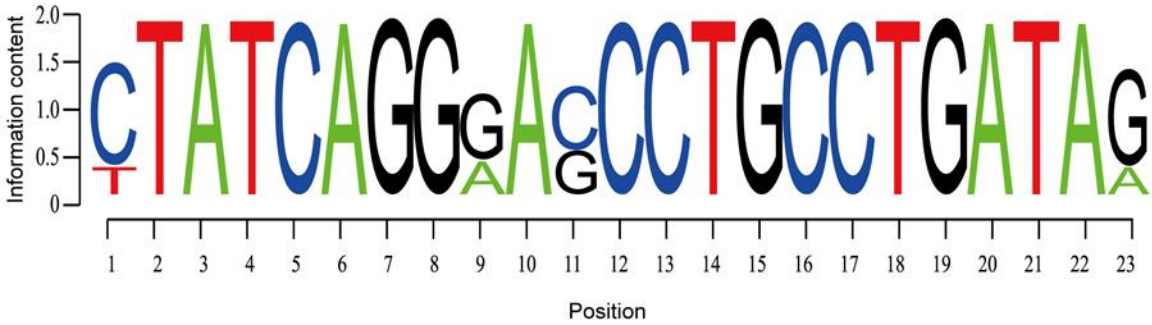

B

Probe RokL6-BS CGCACCGGTAATCCACTATCTATCAGGCAGGCTCCCTGATAGTTTACGCCGCGGATTGAC

→ ***rokL6*-IR** ←

Probe RokL6-M1 CGCACCGGTAATCCACTATCGAATTCGCAGGCTCCCTGATAGTTTACGCCGCGGATTGAC

*Eco*RI

Probe RokL6-M2 CGCACCGGTAATCCACTATCTATCAGGCAGGCTCCGAATTCGTTTACGCCGCGGATTGAC

*Eco*RI

Probe RokL6-M3 CGCACCGGTAATCCACTATCGAATTCGCAGGCTCCGGATCCGTTTACGCCGCGGATTGAC

*Eco*RI *Bam*HI

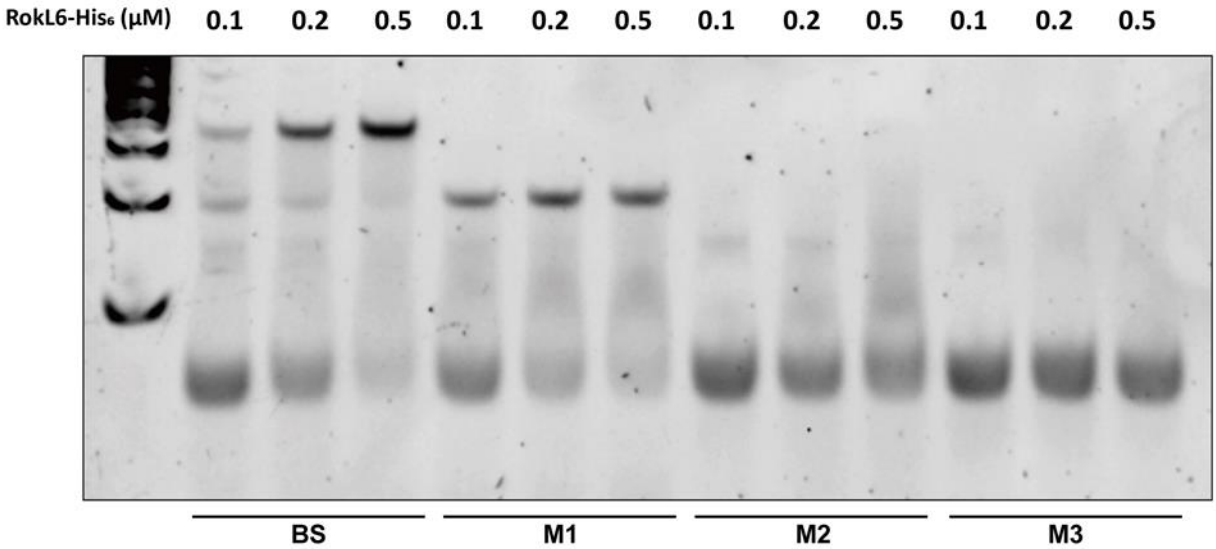

Figure 5

A

SCO1448

-35

5′GGGCATGCCGGGATCCTTCCAGATCGGCGGCGCGGGGGCCGCACCGGTAATCCACTATCTAT

3′CCCGTACGGCCCTAGGAAGGTCTAGCCGCCGCGCCCCCGGCGTGGCCATTAGGTGATAGATA

-10

SCO1448 TSS

CAGGCAGGCTCCCTGATAGTTTACGCCGCGGATTGACGGACACGGAGGGGTGGACCATGAAC 3′

GTCCGTCCGAGGGACTATCAAATGCGGCGCCTAACTGCCTGTGCCTCCCCACCTGGTACTTG 5′

rokL6 TSS

-10

-35

rokL6

start codon

-10 or -35 box

RokL6 binding site

TSS

transcription direction

B

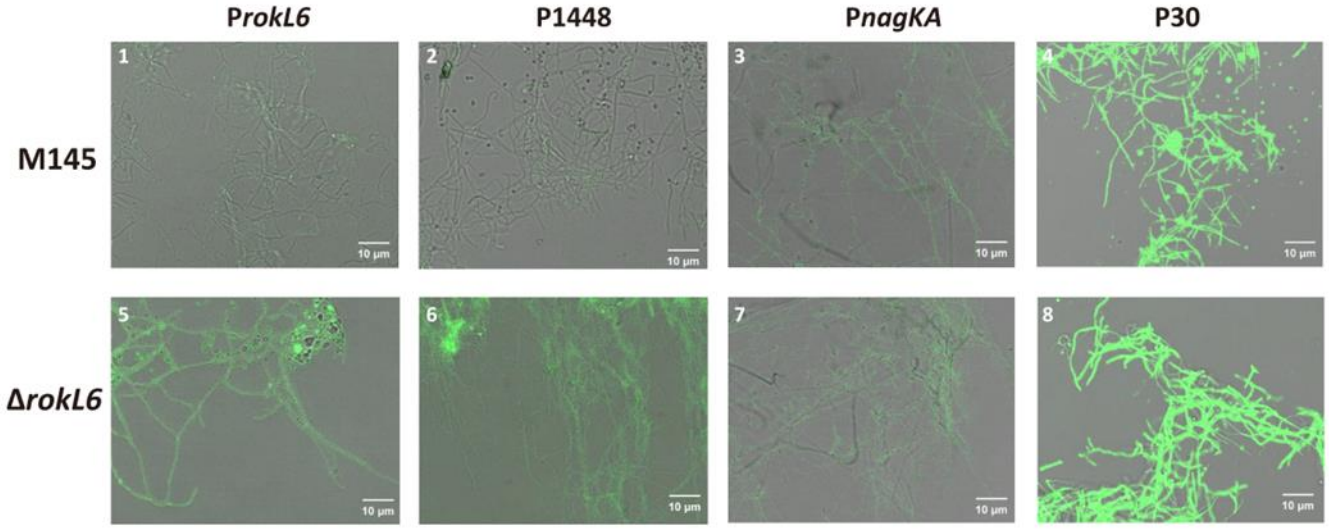

C

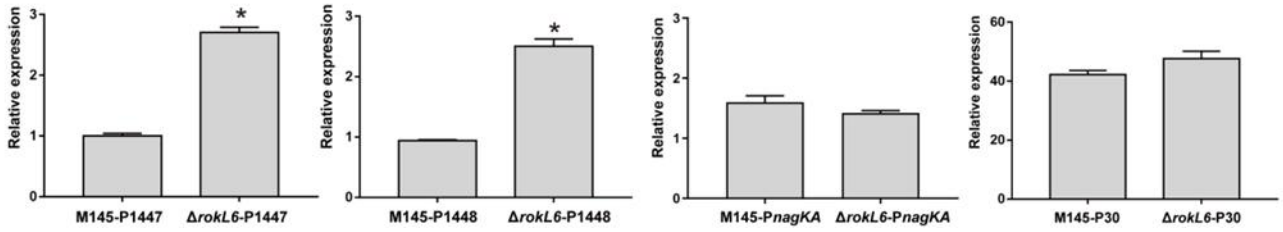

Figure 6

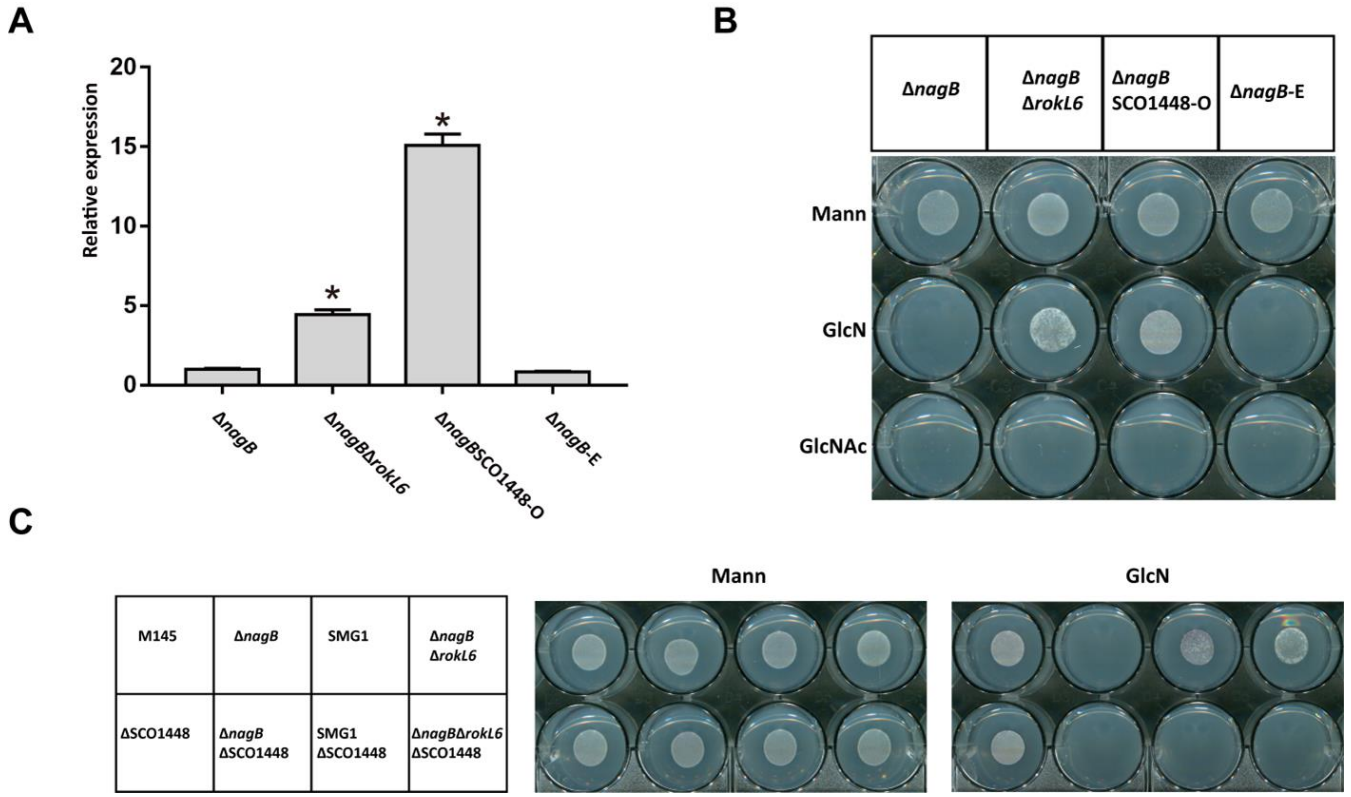
A
Relative expression
20
15
10
5
0
*
*
ΔnagB
ΔnagBΔrokL6
ΔnagBSCO1448-O
ΔnagB-E
B
ΔnagB
ΔnagB ΔrokL6
ΔnagB SCO1448-O
ΔnagB-E
Mann
GlcN
GlcNAc
C
M145
ΔnagB
SMG1
ΔnagB ΔrokL6
ΔSCO1448
ΔnagB ΔSCO1448
SMG1 ΔSCO1448
ΔnagBΔrokL6 ΔSCO1448
Mann
GlcN

Figure 7

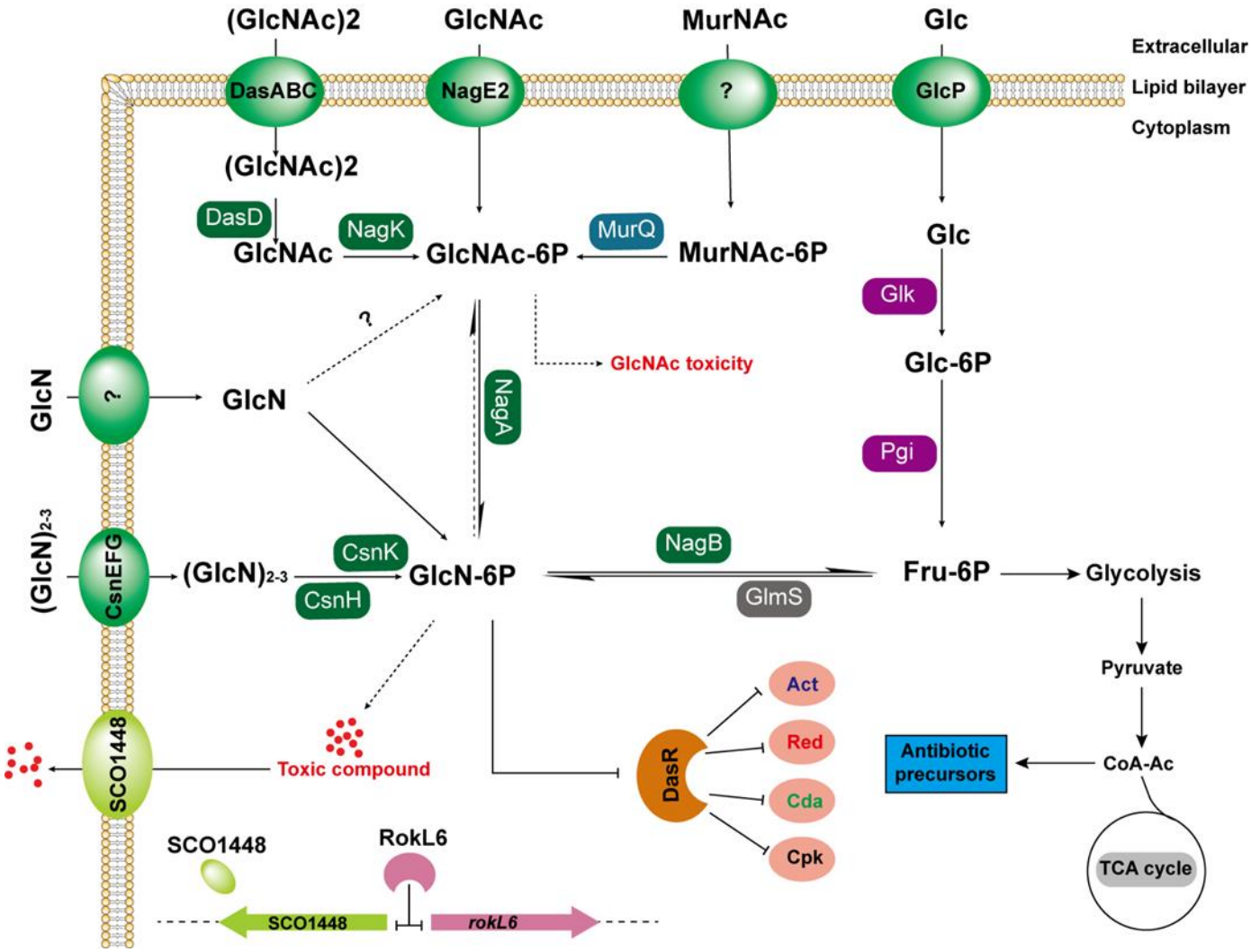
(GlcNAc)2
GlcNAc
MurNAc
Glc
Extracellular
Lipid bilayer
Cytoplasm
DasABC
NagE2
?
GlcP
(GlcNAc)2
DasD
NagK
MurQ
GlcNAc
GlcNAc-6P
MurNAc-6P
Glc
Glk
Glc-6P
Pgi
GlcN
?
GlcN
NagA
GlcNAc toxicity
(GlcN)2-3
CsnEFG
(GlcN)2-3
CsnK
CsnH
GlcN-6P
NagB
GlmS
Fru-6P
Glycolysis
Pyruvate
CoA-Ac
TCA cycle
Antibiotic precursors
SCO1448
Toxic compound
DasR
Act
Red
Cda
Cpk
SCO1448
RokL6
SCO1448
rokL6

Figure 8